Paper 253

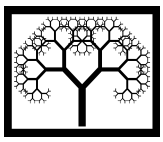

Proceedings of the Tenth International Conference
on Computational Structures Technology,
B.H.V. Topping, J.M. Adam, F.J. Pallarés,
R. Bru and M.L. Romero, (Editors),
Civil-Comp Press, Stirlingshire, Scotland

Comparison of Different Finite Element Models for the Transient Dynamic Analysis of Laminated Glass for Structural Applications

J. Barredo[1], M. Soriano[2], L. Hermanns[2], A. Fraile[2] M. López[3] and M.S. Gómez[2]
[1] Centre for Modelling in Mechanical Engineering (CEMIM-F2I2)
[2] Department of Structural Mechanics and Industrial Constructions
Polytechnical University of Madrid, Spain
[3] University of Oviedo, Gijón, Spain

Abstract

Commercial laminated glass is usually composed of two glass layers and an interlayer of PVB. The viscoelastic behaviour of the PVB layer has to be taken into account when dealing with dynamic loads. This paper shows different Finite Element (FE) models developed to characterize laminated glass. Results are contrasted with data from different reference test cases. First, a quasi-static test is reproduced with a 2d model through a transient analysis. In addition, flexural modes of vibration in a free-free test configuration have been analysed using 2d as well as 3d FE models. Apart from using transient analysis in order to simulate the dynamic behaviour of laminated glass, an iterative procedure has been employed which permits to identify the correct value of the shear modulus of the PVB layer for each mode in an eigenvalue analysis.

Keywords: laminated glass, viscoelasticity, temperature dependency, frequency dependency, simplified numerical models, iterative modal identification, PVB.

1 Introduction

As a result of its increasing importance, many improvements have been made since laminated glass was invented. Its increasing popularity comes from its multiple uses as it can be applied for many safety and security needs, varying only its thickness. Commercial samples are usually composed of two or more glass layers with a thickness of either 2.9 mm or 3.8 mm and an interlayer of polyvynil butiral (PVB from now on) 0.38 mm thick, but more layers can be added to produce stronger glass. While commercial thicknesses can be sufficient for many applications such as curtain walls or windshields, additional layers of PVB and glass are used to obtain the increased strength needed for bulletproof products.
Thus, it turns out to be necessary to model this composite material with such interesting characteristics for human safety and security for design purposes [1].

While the static behaviour is well understood and several design codes like [2] are available, the dynamic response of laminated glass is an important research topic due to its complex nature. In the context of dynamic analysis glass can be considered as a linear elastic material while PVB is considered to behave viscoelastically. The time dependent viscoelastic properties imply transient dynamic analyses in order to represent stress relaxation and creep. The PVB layer is generally almost ten times thinner than the glass layers leading to finer meshes so as to obtain well-shaped elements. Hence, models become more intricate and calculation times increase notoriously.

2 Objective

The computer time needed to run 3D models is very large and consequently their use is normally limited to benchmark studies. For this reason these models are impractical for parametric studies even though they return reliable results that agree with those from different reference test cases.
Therefore, the paper's main objective is to represent the mechanical behaviour of laminated glass subjected to dynamic loads with simplified models that return results of reasonable accuracy but requiring shorter simulation times. A comparison will be made throughout the paper between the different models proposed.

3 Material characterisation

3.1 Glass characterisation

Even though there are many different types of glass, it may be considered a homogeneous, isotropic and linear elastic material within the range of time scales and temperatures considered throughout this paper. The most important properties of the particular type of plane glass used in the benchmark cases are listed in Table 1.

Young's modulus	Poisson's ratio	Density
E=72 GPa	ν=0.22	ρ=2500 kg/m^3

Table 1: Glass properties

3.2 PVB characterisation

PVB is both time and temperature dependent; thus, it is considered as a linear viscoelastic material. The time-dependent response is characterised by separated volumetric and deviatory terms, being the first characterised by the bulk modulus K whereas the shear modulus G reflects the deviatory behaviour. This is shown in Equation (1). Here ϵ_v and ϵ_d are, respectively, the volumetric and deviatory strain tensors.

$$\sigma(t) = \int_{-\infty}^{t} K(t-\tau)\frac{d\epsilon_v(\tau)}{d\tau}d\tau + \int_{-\infty}^{t} 2G(t-\tau)\frac{d\epsilon_d(\tau)}{d\tau}d\tau \quad (1)$$

The bulk modulus of PVB is considered to be constant throughout this study. The shear modulus can be represented by a Prony series as shown in equation (2).

$$G(\tau) = G_0\left[\alpha_\infty^G + \sum_{i=1}^{n_G}\alpha_i^G e^{-\frac{\tau}{\tau_i^G}}\right] \quad (2)$$

More information about the modelling of viscoelastic material behaviour can be found in standard text books like [3],[4],[5],[6] and [7]. Parameters of the Prony series have been obtained by means of testing PVB material. Since the bulk modulus is considered constant, the test has been carried out to determine the Prony series parameters of Young's modulus E and making the necessary transformations to determine the corresponding values of the shear modulus. The tests have been carried out at the reference temperature of 20ºC. Results are shown in Table 2 and 3.

Instantaneous shear modulus	Bulk modulus	Poisson's ratio	Density
G_0=1.19 GPa	K=2 GPa	ν=0.3908	ρ=1030 kg/m^3

Table 2: PVB properties

α_i^G	τ_i^G (s)
0.151	3.09 e-07
0.191	3.08 e-06
0.141	3.07 e-05
0.184	0.0003066
0.139	0.003057
0.122	0.03049
0.054	0.304

α_i^G	τ_i^G (s)
0.0137	3.032
0.00211	30.23
0.000946	301.5
9.65 e-05	3007
0.000275	3.00 e+04
0.000154	2.99 e+05

Table 3: Prony series parameters at a reference temperature of 20ºC

Temperature dependence has been characterised using one of the most commonly used shift functions: the Williams-Landel-Ferry shift function (WLF from now on), which is shown in Equation (3) [3]. WLF constants are given in Table 4.

$$\log_{10}\left[A(T)\right] = -\frac{C_1\left(T - T_{ref}\right)}{C_2 + T - T_{ref}} \quad (3)$$

WLF constants		
C_1	C_2	T_{ref}
49.806	328.46	20ºC

Table 4: WLF shift function constants

Time and frequency dependency of the shear modulus is represented in Figures 1 and 2, respectively.

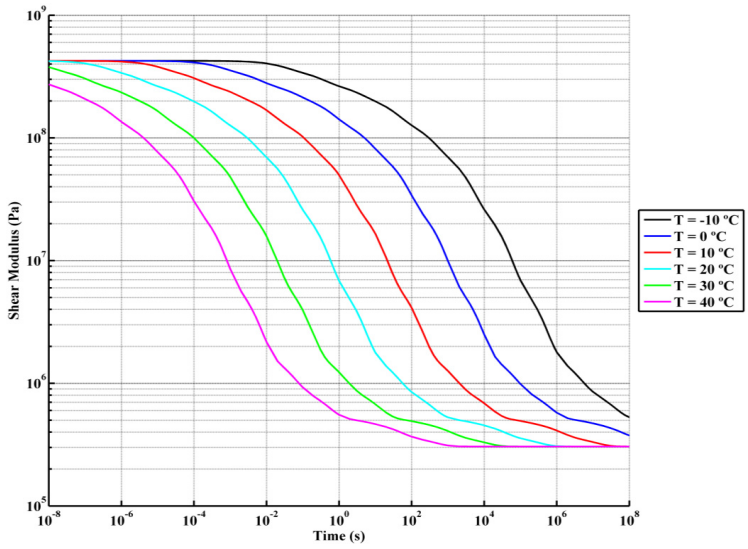

Figure 1: Shear modulus vs. time at different temperatures

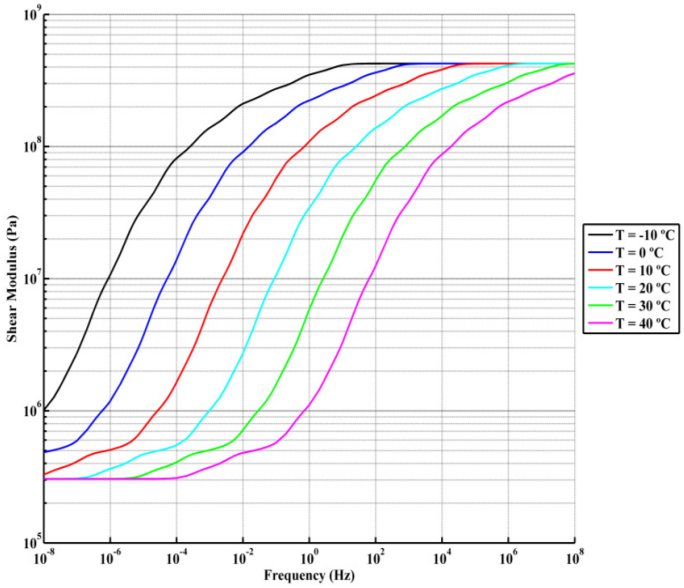

Figure 2: Shear modulus vs. frequency at different temperatures

4 Quasi-static analysis

Previous to the modal analysis, a quasi-static test has been simulated in order to verify the simplified 2d model. To this end, a four line bending test has been employed applying displacements at very low speed. As the time dependency of the shear modulus of the PVB layer may not be neglected, a transient analysis has been

prepared and the behaviour of the PVB and the glass has been compared with the test results.
In what follows, the tests and the model are described in detail.

4.1 Test description

A four point bending test has been carried out on a 8mm thick laminated safety glass sample with a 0.76mm PVB layer, 100mm wide and 300mm long. A similar test setup as the one proposed by European Standard EN 1288-1:2000 [7] was used nevertheless this Standard refers to plane monolithic glass. On Figures 3 and 4 the way in which the sample has been placed for testing is shown.

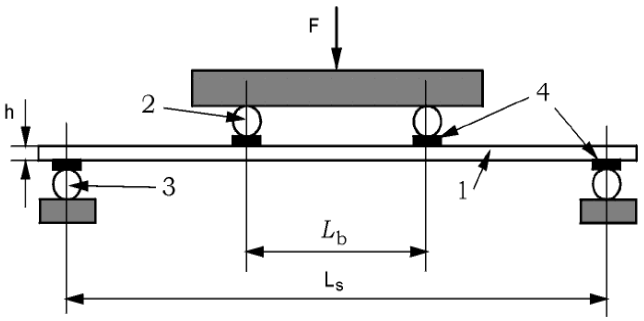

1. Sample
2. Bending roller
3. Support roller
4. Rubber band

L_b = 200 mm
L_s = 250 mm

Figure 3: Four point bending test description

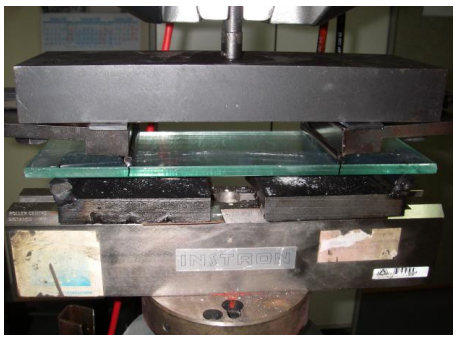

Figure 4: Real test setup

In order to measure flexural deformations, two strain gauges have been placed: the first one (gauge G1) in the centre of the plate and the second one (gauge G2) 65 mm away from gauge G1. Figure 5 shows the positions of these gauges.

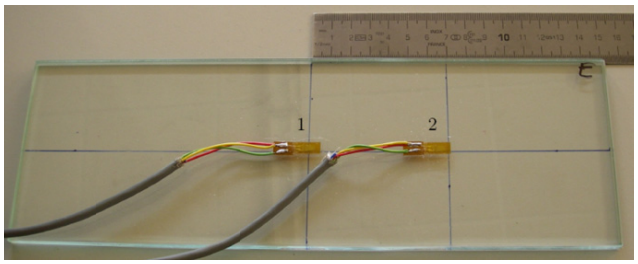

Figure 5: Position of the strain gauges

4.2 Description of the plane Finite Element model

A plane strain model has been employed to simulate the test. This type of model permits both very fine meshes and reduced calculation times. A high-order two-dimensional 8-node plane element that exhibits quadratic displacement behaviour has been used. Symmetry conditions have been applied. Nine elements along the height of the plate have been chosen using three elements for each layer. Contact between the sample and the support rollers has been taken into account. A value of 0.6 for the friction coefficient has been employed according to the literature. In order to avoid convergence problems, the mesh is finer near the contact zone. Figure 6 shows a detail of the mesh near the contact points.

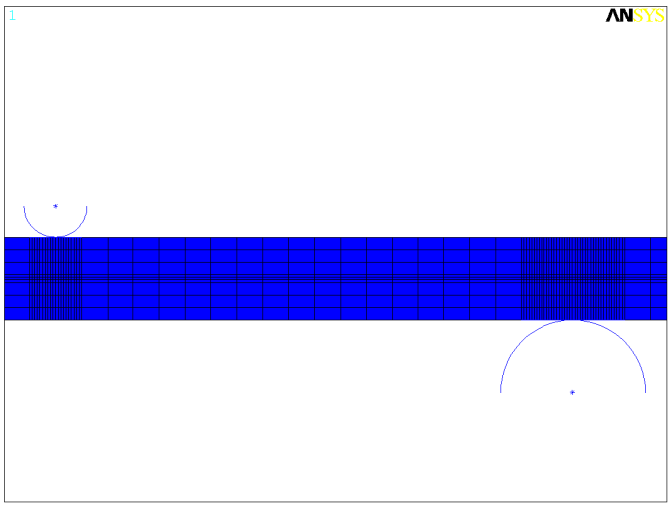

Figure 6: Detail of the contact region

The calculation has been carried out taken into account the test conditions in the laboratory. In this case, the temperature was 22ºC and the displacement was applied at a rate of 0.016 mm/second.

4.3 Results comparison

The load-displacement curve obtained from the test machine and the numerical model is compared in Figure 7. The stiffness of the test machine is determined by a calibration process. The additional displacements during the test have been added to the numerical results before comparing experimental and numerical results.

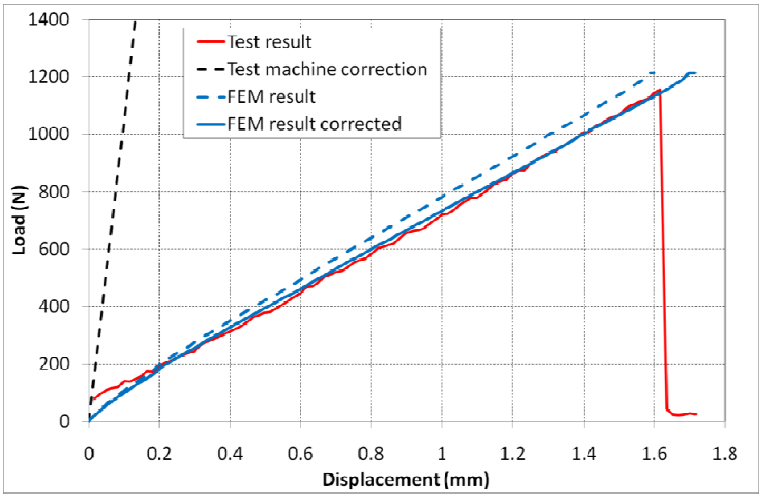

Figure 7: Load vs. displacement curve

An initial preload was imposed in the test. This effect is not reflected in the numerical model since the main objective consists in matching the slope of the load-displacement curve.
Comparison in terms of load vs strain avoids introducing the test machine stiffness. Results obtained from the test and the numerical models may thus be directly compared.

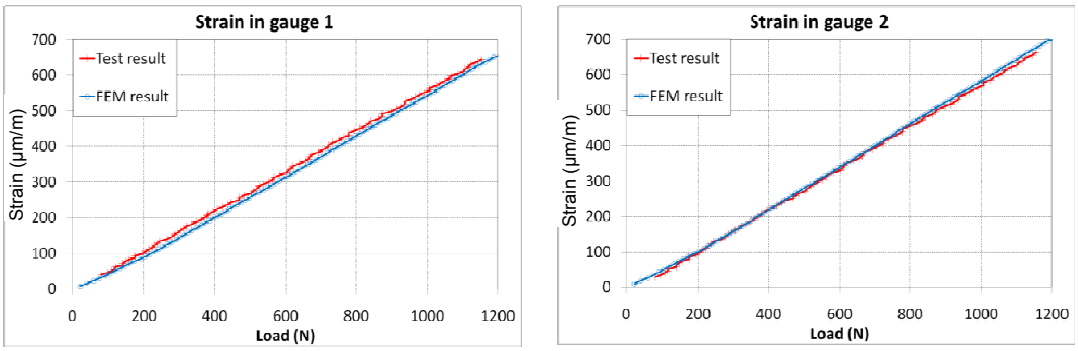

Figure 8: Strain vs. load curves

The stress distribution in the centre section of the sample reveals that the two glass layers behave almost like two separated plates. Both of them are under compression at their respective tops and under traction at their bottoms. The stress distribution in

the PVB layer is determined by the boundary values at the interfaces with the glass layers i.e. its top is under traction while the bottom is compressed as may be appreciated in Figure 9.

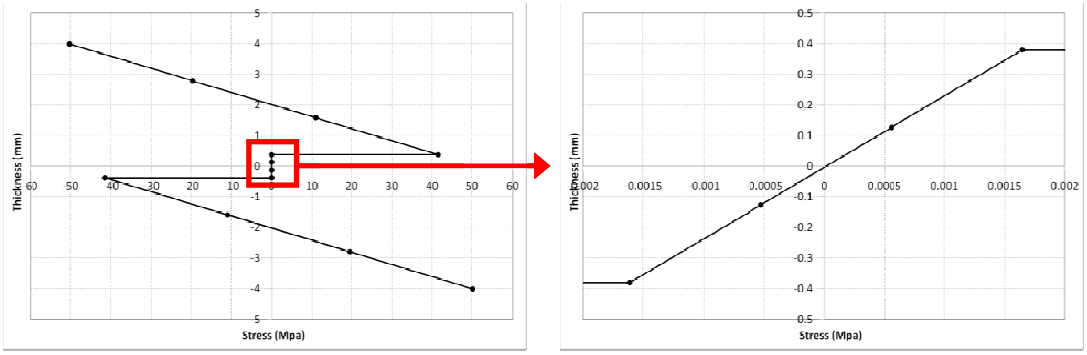

Figure 9: Stress distribution along the height of the test specimen

Since the model behaves quite well and the agreement with the test results is satisfactory, the next step taken consists in using this simplified model to analyze a more sophisticated test.

5 Modal identification

5.1 Test description

For the modal identification, a free-free test case has been carried out. The test specimen was supported by means of two strings and has been randomly excited with a pen in time, space and intensity. Figure 10 illustrates the tested configuration.

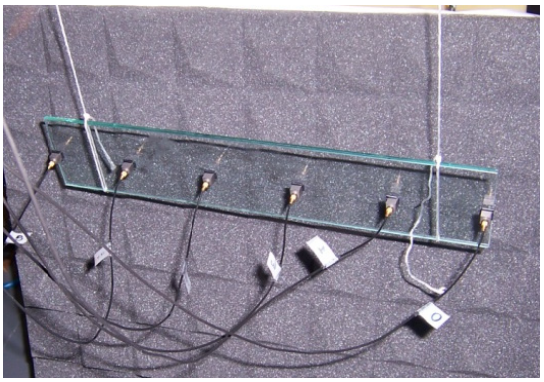

Figure 10: Free-free test configuration

Characteristics of the sample are detailed in Table 5.

Length (mm)	Width (mm)	Thickness (mm)	Accelerometers
500	100	3+0.38+3	6

Table 5: Sample characteristics

The six accelerometers have been equidistantly spaced along the centre line of the test specimen, thus allowing only identification of bending modes.
Mean results from several tests employing the stochastic subspace identification method (SSI) are condensed in Table 6.

Mode	f_n (Hz)	ζ (%)
1	130.78	1.103
2	354.47	1.629
3	690.86	2.989
4	1106.86	3.430

Table 6: Results obtained with the SSI method

5.2 Iterative modal identification

As a first approach for modal identification, an iterative procedure has been applied taking into account the frequency dependency of PVB's shear modulus. The value of the shear modulus is chosen for each target modal frequency. Afterwards, a finite element modal analysis is done and the corresponding modal frequency of interest is compared to the one for which the shear modulus had been chosen. If the absolute difference between both of them is greater than 10^{-3} Hz, the shear modulus is readjusted. The process is then repeated for each mode and sample. The flow chart on Figure 11 will clarify the process.

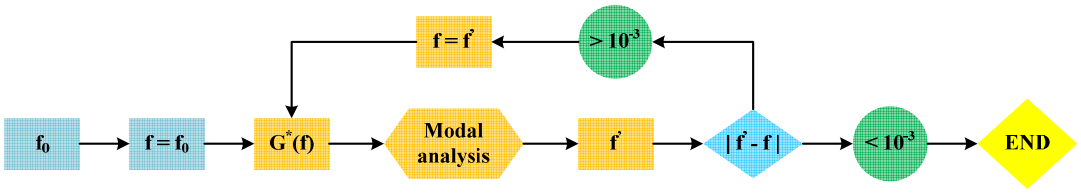

Figure 11: Iterative modal identification flow chart

Consequent to the process, simulation times need to be small enough to make the iterative modal identification feasible. As a result, a three-dimensional solid model with a coarse mesh has been employed.
In this model the entire sample is meshed with 20 elements along the length and 4 along its width. One element is used for each of the three layers. This mesh is selected as it returns very similar results as those extracted from another three-dimensional finite element model with a much finer mesh, requiring only 5 seconds per iteration instead of 10 minutes.

A high order three-dimensional 20-node solid element that exhibits quadratic displacement behaviour is chosen. Each node has three degrees of freedom: translations in the nodal directions x, y and z.
In order to model the two strings that support the sample, a uniaxial tension-only three-dimensional spar element is selected. With the tension-only option, the stiffness is removed during transient dynamic analyses if the element goes into compression. To represent the influence of the accelerometers, structural masses are used. The geometry and imposed boundary conditions are illustrated in Figure 12.

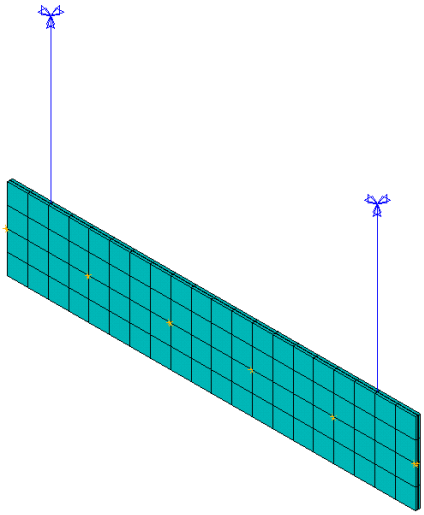

Figure 12: Geometry and boundary conditions of the 3d solid model

Results comparison in terms of natural frequencies is shown in Table 7. The relative difference ε_{fn} between experimental and numerical results regarding the natural frequency is defined in Equation (4).

$$\varepsilon_{f_n} = \frac{\left| f_{n_{test}} - f_n \right|}{f_{n_{test}}} \cdot 100\% \tag{4}$$

Mode	TEST RESULTS	MODAL ANALYSIS	
	f_n (Hz)	f_n (Hz)	ε_{f_n} (%)
1	130.78	133.01	1.71
2	354.47	364.27	2.76
3	690.86	704.19	1.93
4	1106.86	1132.83	2.35

Table 7: Comparison of test and modal analysis results

It can be seen that the iterative modal analysis gives nominal frequency results with errors lower than 3%.

5.3 Transient dynamic analysis

5.3.1 Plane model

Due to the good results obtained for the quasi-static simulations, the plane model has been used to simulate the modal test. As the strings are perpendicular to the plane modelled and a soft spring has been added.
The model has been meshed with 100 elements along the length, 5 along the height of each glass layer and 3 for the PVB layer. A high order two-dimensional 8-node plane element that exhibits quadratic displacement behaviour has been used. Each node has two degrees of freedom: translations in the nodal directions x and y.

To represent the influence of the accelerometers, structural masses have been used. The geometry and imposed boundary conditions are illustrated in Figure 13.

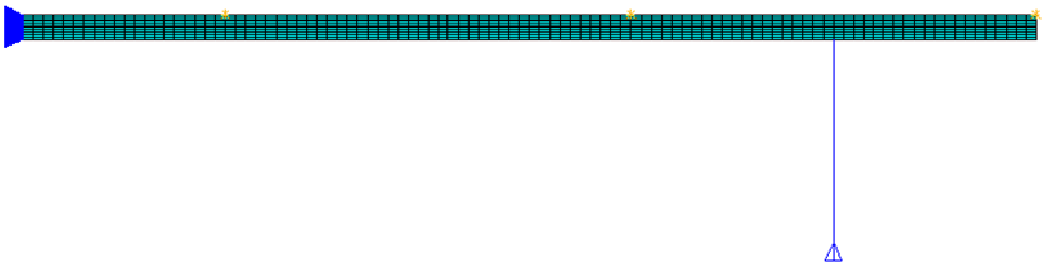

Figure 13: Geometry and boundary conditions of the plane model

An impulsive force has been applied and then the sample has been left to freely respond enough time so that both damping and natural frequencies can be identified. In order to determine what does enough time exactly mean and what time step is really necessary to correctly identify both damping and natural frequencies, a parametric study has been realised. Two variables have been taken into consideration:

- Number of points necessary to describe the highest natural frequency.

$$n = \frac{1}{\Delta t \cdot f_{max}} \tag{5}$$

- Number of cycles during the simulation corresponding to the lowest natural frequency.

$$m = f_{min} \cdot t_{max} \tag{6}$$

To limit the computational effort only the first mode is considered in what follows. Results from this parametric study are gathered on Figures 14 and 15, employing the same identification algorithm as in the test case (SSI).

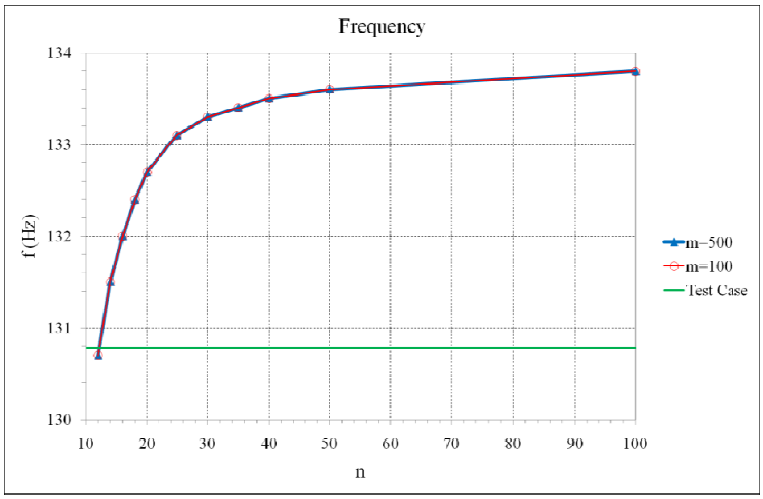

Figure 14: Parametric study for the first mode – Natural frequency

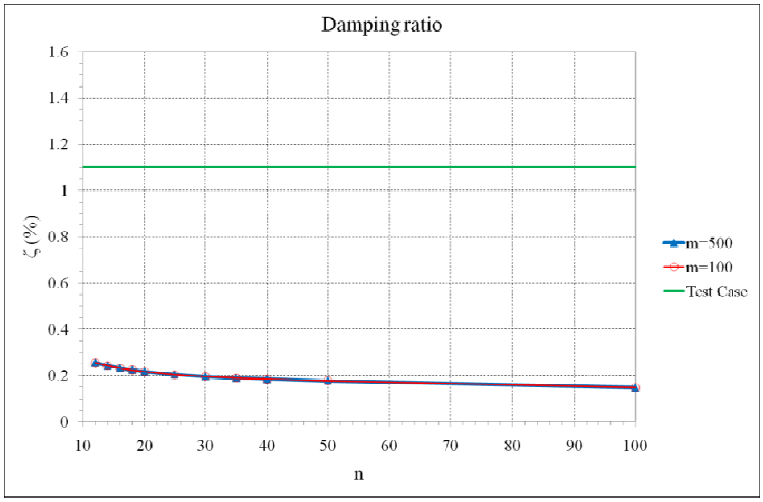

Figure 15: Parametric study for the first mode – Damping ratio

In order to obtain results of reasonable accuracy one cycle should be sampled with at least 30 points. Taking a look at Figure 15 it can be seen that even more points should be used when damping ratios have to be determined with high precision. This value is significantly higher than the lower limit that is stated as rule of thumb in the User Manual of Ansys! According to [9] at least 20 discrete points per period of the highest mode frequency should be used. Thus, to identify correctly both damping and natural frequencies the maximum time step and minimal duration should be chosen as indicated in Equations (7) and (8).

$$\Delta t = \frac{1}{30 \cdot f_{max}} \tag{7}$$

$$t_{max} = \frac{100}{f_{min}} \tag{8}$$

5.3.2 3d solid model

A more sophisticated model is required in order to validate the simplified one. As has been shown before, the plane model estimates quite correctly the first natural frequency using transient dynamic analysis and with the simplified iterative modal analysis the resulting frequencies of the first four bending modes have been determined with relative differences of less than 3%. While the frequencies may be determined to within acceptable errors, the differences between the obtained damping values are very large. Therefore, a 3d solid model has been employed in order to confirm the damping ratios obtained with the plane model.

The calculation has been focused on the first natural frequency in order to limit computer time. For the same reason the recommended number of cycles has been slightly relaxed to 80 instead of 100. On the other hand the number of time steps per cycle has been chosen to be 60 in order to increase the precision of the identified damping values.

As the study has been focused on the first natural frequency, a symmetric model that considers half of the test specimen is sufficient for the identification.

The model has been meshed with 25 elements along the length and 10 along its width. Three elements have been used along the thickness of each glass layer and one for the PVB layer.

The influence of the accelerometers has been accounted for by including structural masses.

5.4 Results comparison

Results obtained from the 2d as well as 3d models for the first mode are presented together with the test results in Table 8.

The relative difference ε_ζ between experimental and numerical results regarding the damping ratio is defined in Equation (9).

$$\varepsilon_\zeta = \frac{|\zeta_{test} - \zeta|}{\zeta_{test}} \cdot 100\% \tag{9}$$

	Test results	Iterative Modal Analysis		Transient Analysis			
				Plane model		Solid model	
Mode	f_n (Hz)	f_n (Hz)	ε_{f_n} (%)	f_n (Hz)	ε_{f_n} (%)	f_n (Hz)	ε_{f_n} (%)
1	130.78	133.01	1.71	133.6	2.16	132.9	1.62
	ζ (%)	ζ (%)	ε_{ζ} (%)	ζ (%)	ε_{ζ} (%)	ζ (%)	ε_{ζ} (%)
	1.103	-	-	0.177	83.95	0.09	91.84

Table 8: Damping ratios identified employing SSI algorithm

The results obtained from the 3d solid model confirm those obtained with the 2d models demonstrating that the simplified models behave in a correct way.

The three methods employed to determine the natural frequencies return acceptable results being the relative difference between experimentally and numerically obtained values always below 3%. However, the damping ratio shows similar differences for both 2d and 3d models with regard to the test results. Therefore, it seems that these models do not reflect adequately the damping mechanisms present during the tests.

Further investigations are being carried out in order to clarify this issue. On one hand, it may be possible that the damping of the glass layers has to be taken into account. On the other hand, it's also thought that the accelerometer cables introduce some amount of damping which may be important considering the generally low damping ratios. To check this, more tests are going to be carried out eliminating the cables and measuring displacements by means of a laser device.

6 Conclusions

Different laminated glass tests have been simulated with the FE method in order to investigate the influence of important parameters like the time step size or duration of the numerical simulation on the values obtained for natural frequencies and damping ratios. The results obtained indicate that the number of cycles during the simulation should be at least 100 while it is recommended that the number of time steps per cycle should be at least 30. The latter value should be increased when damping values have to be determined with high precision. Using a smaller time step leads to higher values for the identified frequency and to lower damping ratios.

It has been shown that even quasi-static tests have to be simulated by means of transient analysis as the time dependency of the PVB layer is important. It is of primary importance to account for all environmental factors which affect the material properties during the tests like temperature variations.

The results obtained show that the 2d models may be used for the identification of bending modes or the simulation of the four point bending test. This is particular interesting when using iterative procedures or performing parametric studies as computer time is crucial in these cases. An iterative procedure has been presented to estimate the natural frequencies taking into account the frequency dependence of the shear modulus of the PVB layer.

To identify damping ratios a free-free test configuration has been used. The test specimen has been excited randomly by a pen and the acceleration time histories have been analysed with the SSI method. The test has been simulated with 2d and 3d models and with both types of models the natural frequencies could be identified with reasonable accuracy. However, a quite big difference exists between experimentally and numerically obtained damping ratios. It is thought that the FE models do not include all the dissipative mechanisms that worked during the tests like for instance the damping of the glass layers or the accelerometer cables. Further studies are necessary to clarify this issue.

Acknowledgements

This work has been made under the sponsorship of the University State Secretary, belonging to Spanish Ministry of Science and Innovation, in its contract BIA2008-06816-C02-02. The presented results have been obtained in cooperation with Universidad de Oviedo.

References

[1] M. A. García Prieto, “Dimensionamiento probabilístico y análisis experimental de vidrios en rotura”. Doctoral thesis, 2001.
[2] ASTM E1300 - 09a Standard Practice for Determining Load Resistance of Glass in Buildings
[3] R.S. Lakes, “Viscoelastic materials”, Cambridge University Press, New York, USA, 2009
[4] R.M. Christensen, “Theory of viscoelasticity”, Dover Publications Inc, New York, USA, 1982.
[5] D.I.G. Jones, “Handbook of viscoelastic vibration damping”, John Wiley & Sons Ltd, West Sussex, England, 2001.
[6] W.N. Findley, J.S. Lai, K. Onaran, “Creep and relaxation of nonlinear viscoelastic materials”, Dover Publications Inc, New York, USA, 1989.
[7] W. Flügge, “Viscoelasticity”, Blaisdell Publishing Company, Waltham, Massachusetts, USA, 1967.
[8] UNE- EN 1288-3:2000 Vidrio para la edificación - Determinación de la resistencia a flexión del vidrio -Parte 3: Ensayos con probetas soportadas en dos puntos (flexión 4 puntos).
[9] ANSYS 12.1 Structural Analysis Guide: 5.9.1 Guidelines for Integration Time Step